HARD X-RAY SOURCE PROFILES AS DETERMINED BY RHESSI

E. J. Schmahl [1], and G. J. Hurford[2]

[1] *Astronomy Department, University of Maryland, College Park, MD 20742, USA*
[2] *Space Sciences Lab, University of California, Berkeley, CA 94720, USA*

ABSTRACT

The Reuven Ramaty High Energy Solar Spectroscopic Imager (RHESSI) has been recording rotationally-modulated X-rays from solar flares since its launch on February 5, 2002. Its 9 grid pairs time-modulate the detected photon flux giving RHESSI spatial information on hard X-rays at 9 logarithmically spaced angular scales ranging from 2.3 to 183 arcsec. Using the calibrated modulation profiles for a variety of flares, we present new information on the spatial profiles of the hard X-ray structures in flares. We find that the FWHM of cores of single-component flares range from 3 to $11''$ in size. Most of the flares in this set show extended emission out to 2 to 3 times the radii of the cores, and these 'halos' contain up to 25% of the total flux.

INTRODUCTION

The Ramaty High Energy Solar Spectroscopic Imager (RHESSI), was launched in February 2002 with the objective of studying energy release and particle acceleration in solar flares. RHESSI does imaging-spectroscopy of solar hard X-rays and gamma-rays over a 3-keV to 17-MeV energy range using high-purity Germanium detectors and a Rotational Modulation Collimator (RMC) system which encodes spatial information by rapidly time-modulating the observed X-ray flux. Nine subcollimators, with logarithmically spaced angular resolution from 2.3 to 183 arcseconds, provide information on a wide range of size scales. In similar energy bands, this enables RHESSI to resolve sources smaller than the typical $\sim 8''$ minimum FWHM that were reported by previous hard X-ray telescopes (HXIS, Hinotori and Yohkoh/HXT) (*e.g.* Masuda 2002, Sakao, Kosugi and Masuda, 1998). The RHESSI mission is described in detail by Lin *et al.* (2002).

Recently, Schmahl and Hurford (2002) performed a study of RHESSI flares with simple shapes and time profiles and applied unpixelized forward-fitting methods to obtain the size and spatial profiles of the hard X-ray sources. This technique is sensitive to both the small scales ($< 10''$) and the large scales ($> 30''$), and the authors found evidence for both small scale *cores* and large scale *halos* in hard X-ray flares.

The unpixelized forward-fitting technique used earlier, while powerful and fast, does not afford the user much insight into the mechanism by which sizes are determined. This led us to re-determine the source size scales by a method that is at once more understandable on a qualitative level and as accurate as forward fitting. The method we use depends on 'back projection', first devised by Mertz *et al.* (1986), studied by Kilner and Nakano (1989), and described in some detail by Hurford *et al.* (2002).

RHESSI Back Projection

At a given instant in time, the response of a RHESSI detector as a function of source location is the 'modulation pattern' of the corresponding subcollimator (SC) rotated to the roll angle for that time. Detected photons are most likely to have come from regions where the modulation pattern has its highest

values. Back projection creates an image by distributing detected photons onto a map in proportion to the modulation pattern. It sums the modulation patterns over the total integration time, weighting each pattern according to the number of photons detected in each small time bin. In distributing flux across the map by this prescription, however, some of it will appear in 'sidelobes'. For the case of a point source, back projection will assign some of the flux to many other points in addition to the true source location. Nevertheless, in all but perverse cases, the greatest concentration of flux will be at the location of the point source. In mathematical terms, back projection is analogous to performing an inverse Fourier transform, and it has nearly all of the same advantages and disadvantages.

Durouchoux *et al.* (1983) described the process by which back-projection maps could be flat-fielded and normalized. This procedure removes background contributions from the image. With this normalization adapted to RHESSI, the peak of the back-projection map equals the strength of a dominant source. The map then has units of counts $cm^{-2}s^{-1}$, uncorrected for mean grid transmission. This equivalence between the peak of the map and the source strength is strictly accurate only when the source size is small compared to the angular resolution of the subcollimator used for making the map. When this constraint is violated, the source is at least partially 'over resolved', and the amplitude of the modulation (or, in this case, the peak of the back-projection map), is reduced by a factor called the 'relative amplitude'. The relative amplitude depends on the extent to which the source has been over resolved by the subcollimator. When background is negligible, the relative amplitude (ρ) for each subcollimator can be inferred from the map peak (B_{max}), the (known) rotationally-averaged probability of photon passage through the grids ($< P_m >$), where m is the pixel number of the map peak, and the total number of counts (C_{total}).

$$\rho = B_{max} \cdot < P_m > / C_{total} \tag{1}$$

Using this equation and single-subcollimator maps of nine selected flares, we have determined the profiles of the relative amplitude $\rho(k)$ as a function of wavenumber k ($k = 2\pi/p$, where p is the angular pitch of the subcollimator).

Relative Amplitude Profiles

For a round source the relative amplitude profile $\rho(k)$ is the Fourier transform of the spatial profile $I(r)$. We have selected only flares whose Clean maps show isolated round sources (see Schmahl and Hurford 2002), so there is azimuthal symmetry in both the radial profile and its transform. We have found the relative amplitude as a function of wavenumber over ranges of wavenumber that satisfy these criteria:

1) The maximum permitted wavenumber corresponds to the finest subcollimator for which the image is not over resolved. A quantitative analysis was performed to make this determination: The point spread function (PSF) was cross-correlated with each map. The source was deemed to be over resolved if the maximum cross correlation was below 50%. Three of the 9 flares (03/25, 04/17 and 06/02) were found to have cross-correlation maxima greater than 60% with their respective PSF, and the remainder had maximum cross-correlations of less than 40%. This can be also be determined by eye from the back-projection maps of Figure 1. If the center pixels show a bright source surrounded by (at least partial) rings, the source is not over resolved. For example, for SC-1 three flares with cross-correlation maxima greater than 60% show rings around a central peak. All the other SC-1 maps whose cross-correlation maxima are less than 40% show repetitive structures without rings, or negative values where a maximum might be expected. For the 03/18 flare, the finest subcollimator without over resolution was SC 4 and for the flares of 02/20/09:40 and 06/01 it was SC 3. For the rest, SC 2 was the finest subcollimator without over resolution.

2) The minimum permitted wavenumber is determined by how far the source is from the spin axis. A subcollimator was not used if the source was within 2 angular pitches of the spin axis. (In such cases the centroid of the single-subcollimator map is shifted.) For 3 of the flares, the SC-9 map showed a shift of the centroid relative to the other subcollimators. Similarly, the SC-8 map for 02/20/21:00 shows a shift.

3) The detector must be on for the corresponding wavenumber to be included. For 02/26, detector 2 had been switched off during the flare, so SC-2 maps could not be made, and the finest useful subcollimator is SC 3.

To fill in the gaps between the wavenumbers of the subcollimators, we linearly interpolate (and extrapolate at the high wavenumber end) in the $(k^2, ln(\rho))$ plane, before returning to the (k, ρ) plane. This kind of

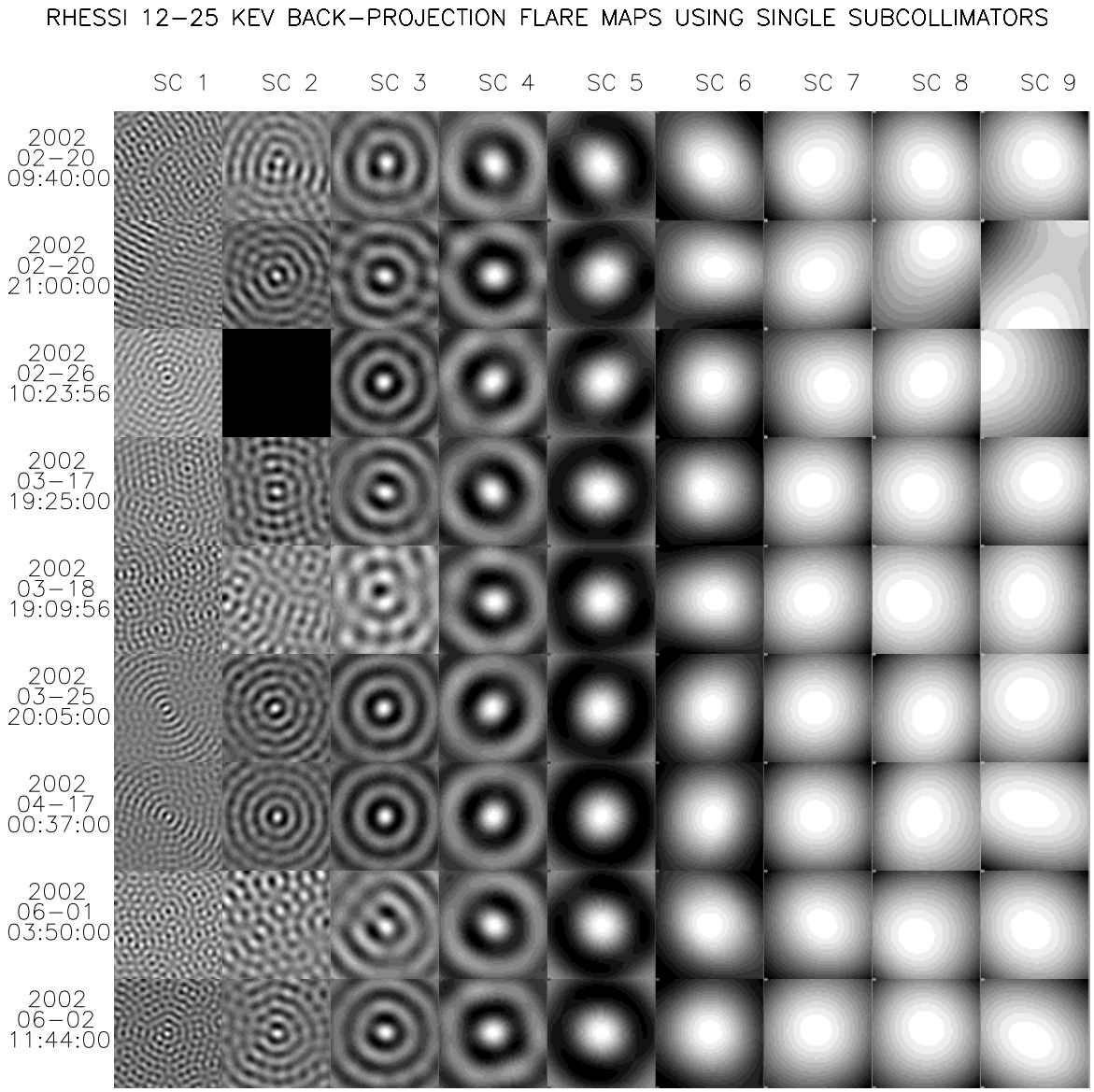

Fig. 1. Back-projection maps in the 12-25 keV band. Each row is for a different flare and each column shows back-projection maps for a single subcollimator (SC) with 1-arcsec pixels, covering a 64x64 arcsec field of view. The rightmost column is for SC 9, whose FWHM is $183''$. All but two of the SC-9 maxima are centered except the second and third flares (02-20 21:00 and 02-26 10:23). This is the result of the source being within ~ 1 angular pitch of the spin axis. The second flare is only $\sim 200''$ from the spin axis, sufficient to affect not only SC-9 but SC-8. As one progresses to finer spatial resolutions, the sidelobes of the modulation pattern begin to appear within the maps. In the column showing SC 3, all but one of the patterns has a bright peak at the center: for the 5th flare (02/03/18), the peak is reversed, indicating 'over resolution', $i.e.$ the source is larger than the angular resolution of SC 3 ($6.9''$). A smaller degree of 'over resolution' may be seen in the SC-3 map of the 8th flare. SC 2 has been included, although it is relatively insensitive below 20 keV. The maps for SC 1, which has $2.3''$ angular resolution show over resolution for all but the 6th, 7th and 9th flares, which evidently have spatial scales approaching $\sim 2.3''$.

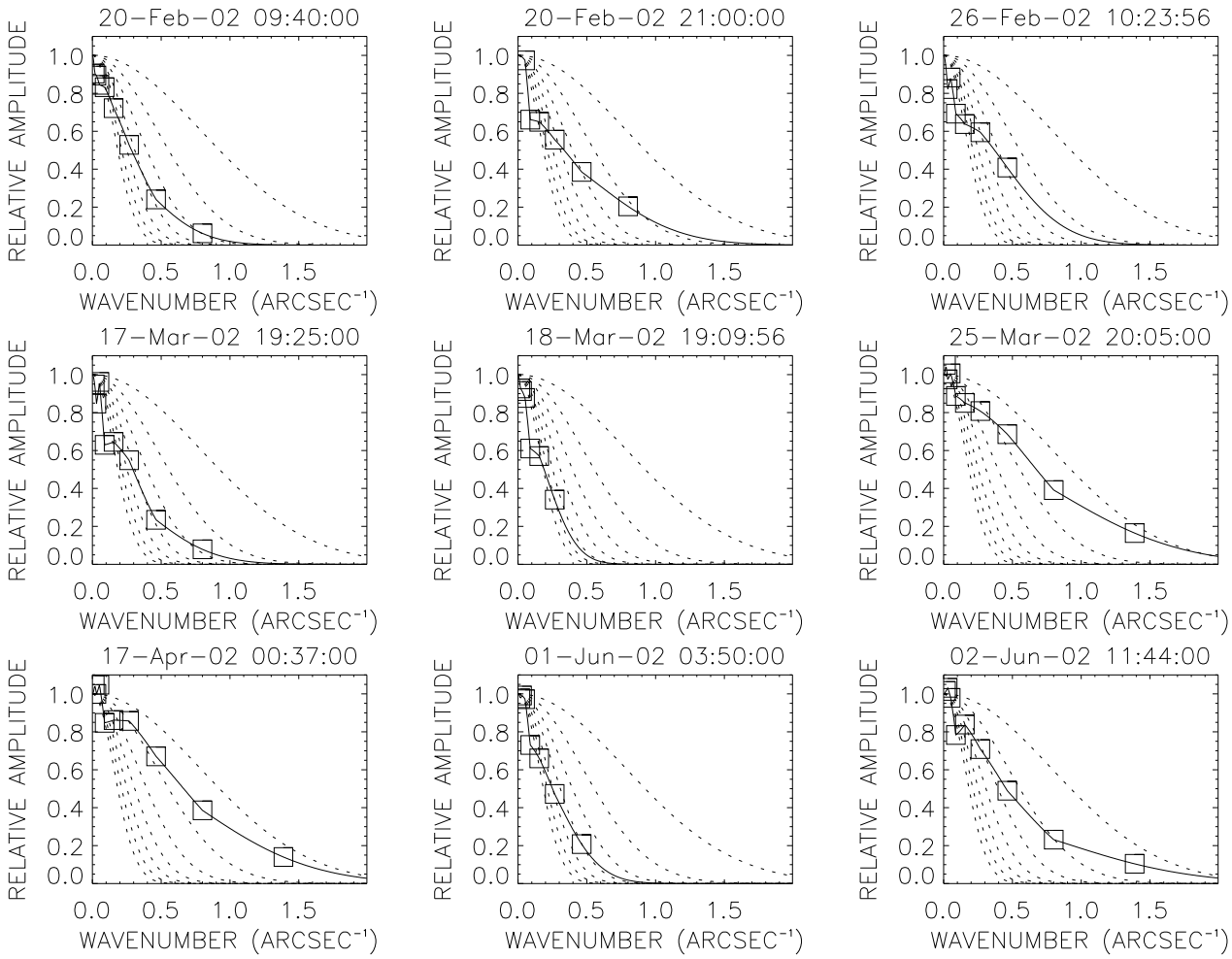

Fig. 2. Relative amplitudes for 9 flares. The nine boxes show the relative amplitudes for different subsets of the subcollimators (see text). The lines through the points are Gaussian interpolations (see text for explanation) which are used to compute the transforms giving the spatial profiles shown in Figure 3. For comparative purposes, the short dashed curves show Gaussian profiles of different FWHMs, illustrating the extent by which these RHESSI profiles depart from Gaussian shapes.

interpolation has three desirable properties: the fit is exact if the profile is Gaussian, the data points are linked smoothly, and no sharp upper cutoffs are created that would yield transform artifacts.

Using the interpolated relative amplitudes $\rho(k)$ for the 9 flares (Figure 2) we then applied the inverse Fourier transform–in this case, a Bessel transform, due to cylindrical symmetry. The resultant spatial profiles, $I(r)$, (light solid curves) are shown in Figure 3. The upper portions of the profiles appear to be approximately Gaussian.

The dashed curves in Figure 3 show the (Gaussian) transforms of the dashed profiles in Figure 2. Departures from the Gaussian shape is illustrated by performing the cumulative flux integral $C(r) = \int_r^\infty I(r) r dr$ (heavy curve in Figure 3), which is also a Gaussian if $I(r)$ is a Gaussian. The difference between $C(r)$ and $I(r)$ gives a measure of the fraction of the flux that is attributable to a 'halo', indicating that, as found our preliminary study (Schmahl and Hurford, 2002), there is significant halo emission.

DISCUSSION AND CONCLUSIONS

Using a new method which combines 'back projection' and transmission probability, we have computed relative amplitude profiles for 9 hard X-ray flares in the 12-25 keV band. Then, making the assumption that their apparent roundness in Clean maps extends to the smallest scales, we determined the source profiles.

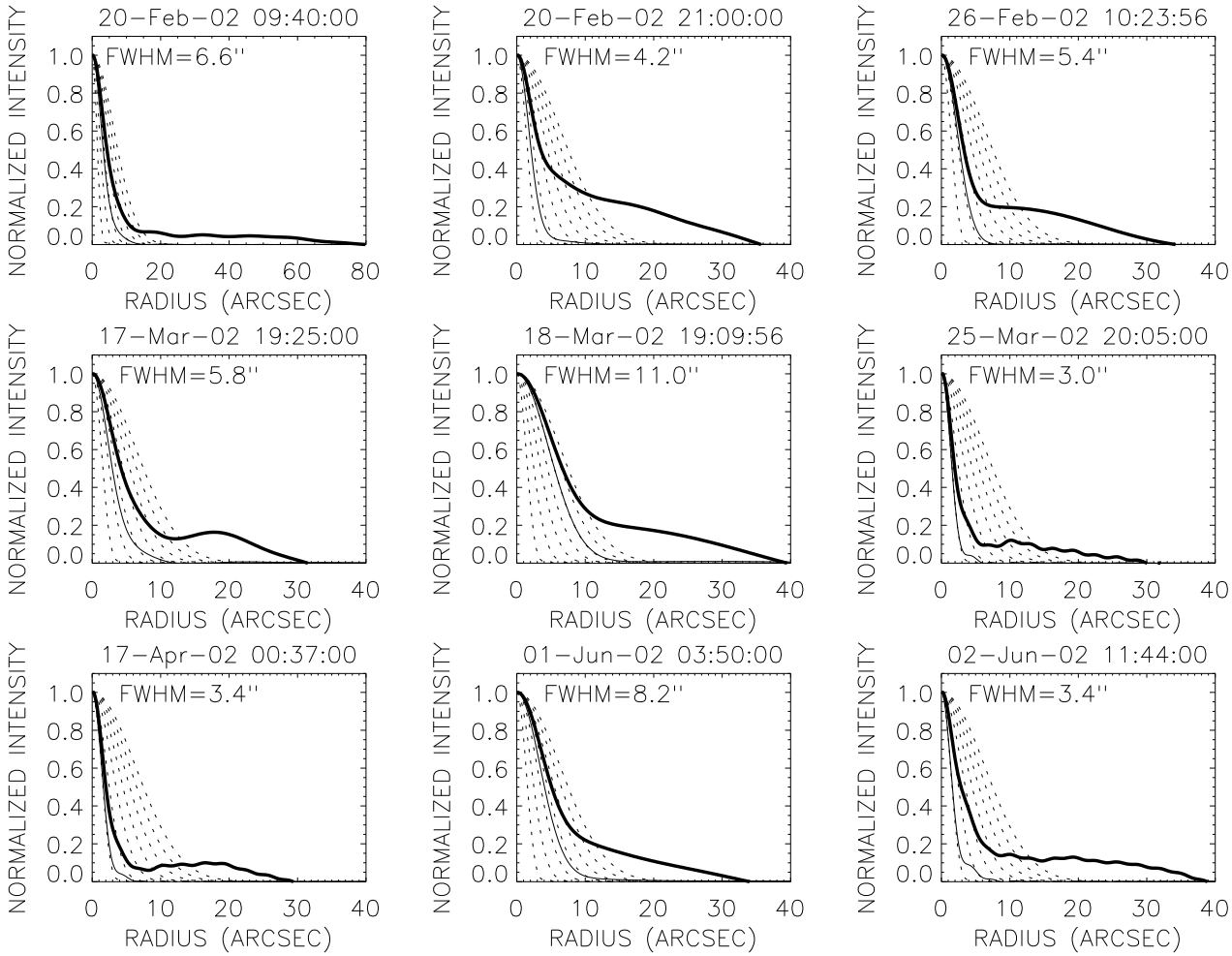

Fig. 3. Spatial profiles inferred for 9 flares. The relative amplitude profiles (Figure 2) were Fourier transformed to obtain the spatial profiles I(r) shown as the light solid curves. Dashed curves show representative Gaussians (FWHM=$3, 5, 7, ..., 15''$) transformed from the dashed Gaussians of Figure 2. The heavy curves show the integrated flux outside the radius. The difference between it and I(r) indicates extended flux beyond the cores.

The results not only provided a robust determination of source sizes from 3 to 11 arcseconds FWHM (Table 1), but also indicated the presence of significant flux outside the flare core. The core sizes found by this method are smaller than those determined by Schmahl and Hurford (2002) using forward-fitting with SC 3-9. In that work, the second finest subcollimator (SC 2) was not used due to doubts about its reliability and also due to a lower energy limit (20 keV). The present study also used an improved technique to compensate for missing spatial frequencies. In the present work, using the 12-25 keV energy band, we have included SC 2, even though its sensitivity is low below 20 keV. This introduces a bias in that the effective energy is higher for SC 2 than the other detectors. Internal evidence, however, indicates self consistency of the relative amplitudes for SC 2: where both SC-1 and SC-3 data exist (3 flares), the values for SC 2 lie on a smooth interpolation between SC 1 and 3. For the other flares, where SC-1 relative amplitudes were effectively zero, the SC-2 data also looks like a reasonable extrapolation from SC 4 and 3. The inclusion of this subcollimator improves the angular resolution dramatically, though the energy dependence of source size scales is unknown.

At this stage in the development of the RHESSI software, it is not possible to say which algorithm, unpixelized forward fitting or back projection, is more accurate for determining spatial scales. Application of forward fitting within the same parameter space as here–finer subcollimators and higher energies– will be necessary before we can assess the consistency of the two methods. Although we have, at present, no

Table 1. Flare Parameters

Date	Time	X-Ray class	Lat/Long	SC #s	Core FWHM	Halo flux
02/02/20	08:40:00	M4.3	N18 W83	2-9	$6.6''$	7%
02/02/20	21:06:00	M2.4	S18 W11	2-7	$4.2''$	25%
02/02/26	10:23:56	C9.6	S13 W89	3-8	$5.4''$	20%
02/03/17	19:25:00	M4.0	S22 E16	2-9	$5.8''$	15%
02/03/18	21:00:00	C8.9	S21 E03	4-9	$11.0''$	20%
02/03/25	20:05:00	C9.8	N08 E17	1-9	$3.0''$	10%
02/04/17	21:00:00	C9.9	S13 W83	1-9	$3.4''$	10%
02/06/01	03:50:00	M1.5	S16 E20	3-9	$8.2''$	20%
02/06/02	11:44:00	C9.4	S17 E09	1-9	$3.4''$	15%

quantitative information about the two-dimensional scales and the degree of elongation in these flares, it is worth pointing out that the assumption of source roundness is not essential. Using superposed-epoch analysis of partial RHESSI rotations, one can extend the method to sources of almost arbitrary shape.

As suggested by Schmahl and Hurford (2002), the 'halo' sources may be manifestations of albedo. If so, then their centroids and sizes should be dependent on the look angle and the height of the primary source. In future work, we plan to study these factors, and compare the halo energy dependence with theoretical models of albedo emission.

ACKNOWLEDGMENTS

One of the authors (EJS) acknowledges support by grant NAG-5-10180 from NASA Goddard Space Flight Center to the University of Maryland. The research is supported by NASA grant NAS5-98033-05/03.

REFERENCES

Durouchoux, P., H. Hudson, G. Hurford, *et al.*, Gamma ray imaging with a rotating modulator, *Astron. Astrophys.* **120**, 150-155, 1983.

Hurford, G. J, E. J. Schmahl, R. A. Schwartz, *et al.* The RHESSI imaging concept, in press, *Solar Physics*, 2002.

Kilner, J. R., and G. H. Nakano, Design studies for X-ray and gamma-ray rotation modulation collimators, Soc. Phot. Inst. Eng. **1159**, *EUV, X-Ray, and Gamma-Ray Instrumentation for Astronomy and Atomic Physics*, 27-33, 1989.

Lin, R. P, B. R. Dennis, G. J. Hurford, *et al.* The Reuven Ramaty high energy solar spectroscopic imager (RHESSI), in press, *Solar Physics*, 2002.

S. Masuda, Hard X-ray solar flares revealed with Yohkoh/HXT, *Multi-wavelength Observations of Coronal Structure and Dynamics*, (Pergamon Press, Amsterdam), Martens and Cauffman (eds.), 2002.

Mertz, L. N., G. H. Nakano, and J. R. Kilner, Rotational aperture synthesis for X-rays *J. Opt. Soc. Am.* **3**, 2167-2170, 1986.

T. Sakao, T. Kosugi, S. Masuda, Energy release and particle acceleration in solar flares with respect to flaring magnetic loops, *Observational Plasma Astrophysics: Five Years of Yohkoh and Beyond*, T. Watanabe *et al.*(eds.), Kluwer Academic Publishers, Boston, Massachusetts), 259-267, 1998.

Schmahl, E. J., and G. J. Hurford, Hard X-ray size scales, in press, *Solar Physics*, 2002.

E-mail address of Edward J. Schmahl schmahl@hessi.gsfc.nasa.gov
Email address of Gordon J. Hurford ghurford@ssl.berkeley.edu